

## Molecular Simulation Study of Nafion Membrane Solvation in Water and Methanol

Aleksey Vishnyakov and Alexander V. Neimark\*

TRI/Princeton, 601 Prospect Avenue, Princeton, New Jersey 08542

Received: October 12, 1999

Molecular mechanics and molecular dynamics simulation studies of conformation and solvation of perfluorosulfate oligomers, representing fragments of Nafion membrane, have been performed. Two typical conformations of the oligomer, composed of 10 monomer units, have been found in a vacuum. A stretched geometry of the fluorocarbon skeleton with tortuosity of 2.4 was reached by energy optimization starting from the regular conformation with all CCCC angles in the trans position. A highly folded spiral-like configuration was obtained when the randomly bent chain was taken as the initial configuration. Molecular dynamics simulations of shorter oligomers solvated in water and methanol revealed a noticeable difference between the geometries of the fluorocarbon skeleton in different solvents. The skeleton structure in water was substantially more folded than in methanol. The side chain of the Nafion oligomers was found to be quite stiff; only a few conformational transitions in the side chain were detected. Both water and methanol formed stable hydrogen bonds with the oxygens of  $\text{SO}_3^-$  group with the hydrogen bond lifetimes several times longer than rotational correlation times of individual solute molecules in the bulk. The other parts of the side chain were found to be hydrophobic, including ester oxygens. On average, each  $\text{SO}_3^-$  group formed ca. five hydrogen bonds to water and four bonds to methanol. The spatial distribution of solvent molecules bonded to the  $\text{SO}_3^-$  group was characterized by a pronounced anisotropic first solvation shell.

## Introduction

Increasing interest in studies of solid polyelectrolytes, such as Nafion membrane, is inspired by their active applications in electrochemistry including water electrolyzers for hydrogen energetics,<sup>1</sup> chlor-alkali technologies,<sup>2</sup> electroorganic synthesis,<sup>3</sup> proton exchange hydrogen and methanol membrane fuel cells, which are seen today as the most promising energy suppliers for vehicles,<sup>4,5</sup> and in separations.<sup>6</sup> Unique engineering properties of Nafion membranes are related to their sufficiently high conductivity and water permeability and, at the same time, efficient blocking action with respect to nonionic components and gases. Electric conductivity of Nafion membranes achieves  $0.01 \Omega^{-1} \text{ cm}^{-1}$ ,<sup>6</sup> while water self-diffusion coefficient at the saturation conditions is only 1 order lower than that in the coexisting bulk liquid.<sup>6,7</sup> In electrochemical applications, Nafion membranes function as an ion-conductive medium and also as a separator of gaseous reactants. In separations, Nafion membranes work as molecular sieves letting through water molecules and blocking transport of organic contaminants and biological agents. Because of high water vapor and air permeability,<sup>8</sup> outstanding chemical, thermal and mechanical stability, small heat accumulation, and reduced weight, Nafion type perfluorinated polymers open new prospects for producing permselective membranes for protective clothing.

Transport and sorption properties of Nafion membranes are determined by polymer microstructure at given environmental conditions. Nafion polymer molecule consists of a poly-(tetrafluoroethylene) backbone and pendant side chain terminated by  $\text{SO}_3^- \text{M}^+$  group (Figure 1). The dried membrane is

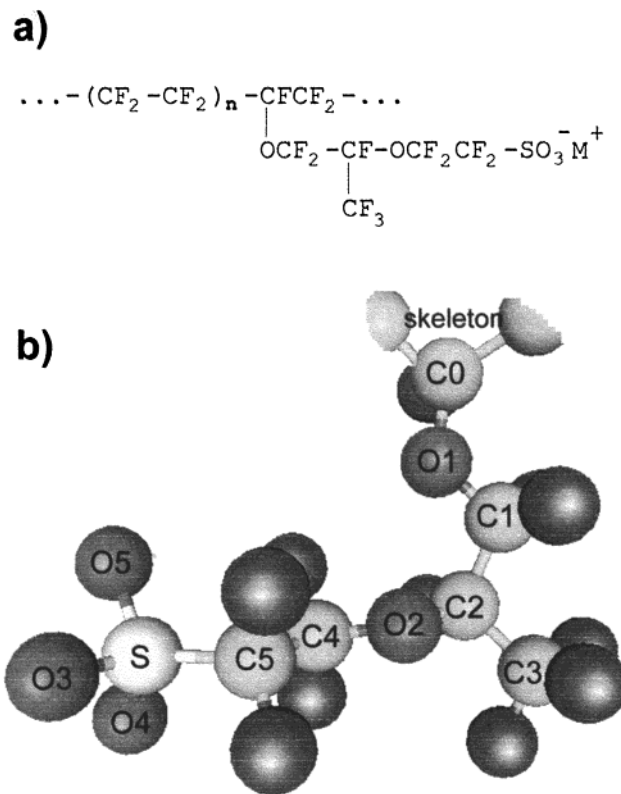


Figure 1. Optimized geometry of the side chain with atom labeling.

able to adsorb substantial amount of water, depending on the equivalent weight of the polymer and the counterion  $\text{M}^+$ .<sup>9,10</sup>

\* Author for correspondence. E-mail: aneimark@tri.princeton.org.

Despite extensive experimental and theoretical studies directed to quantitative characterization of solvated Nafion membranes, little is known about their microstructure on the molecular level. It is well established that Nafion membranes are microheterogeneous, i.e., hydrated Nafion under saturation conditions undergoes microphase segregation. Water molecules and positively charged counterions are supposed to form aggregates or clusters, solvating negatively charged hydrophilic  $\text{SO}_3^-$  groups. These hydrophilic clusters are embedded in the hydrophobic phase of fluorocarbon backbone. On the basis of wide angle and small-angle X-ray diffraction studies, Gierke<sup>9,11</sup> et al. proposed a model of Nafion membrane with spherical water clusters of 30–50 Å in diameter. Water and ions diffuse through pores channeling the hydrophobic backbone. This model was modified by Mauritz and Rogers<sup>12</sup> and recently by Eikerling et al.<sup>13</sup> However, controversial opinions exist regarding the shape and size of the hydrophilic aggregates. According to neutron diffraction studies of Pineri et al.,<sup>14</sup> the size of the water clusters in Nafion under saturation conditions amounts a few tens of nanometers, i.e., they are much larger than those estimated by Gierke et al.<sup>9,11</sup> To the contrary, Falk<sup>15</sup> concluded from an infrared study that the water aggregates are much smaller than estimated by Gierke et al.<sup>9,11</sup> or have a substantially nonspherical shape with frequent intrusions of the fluorocarbon backbone. The authors of<sup>16</sup> found the behavior of hydrated Nafion membrane similar to that of brushlike polymers and suggested a multilayer structure of the hydrated Nafion membrane with lamellar water aggregates. Their assumptions were confirmed by the results of neutron diffraction and Messbauer spectroscopy experiments.<sup>17</sup> On the basis of the X-ray results of Ozerin et al.,<sup>18</sup> Tovbin<sup>19</sup> concluded that the channels in the hydrophobic microphase are ca. 50% wider than those in the model of Gierke et al.<sup>9,11</sup> The molecular structure of water in the aggregates remains enigmatic. IR measurements of Falk<sup>15</sup> revealed less hydrogen bonding in water sorbed to Nafion compared to the bulk liquid. Approximate structures of the solvation shells around  $\text{SO}_3^-$  groups was proposed. An omnipresent question is the influence of the solvent, usually water, on the molecular geometry and dynamics of conformational transitions in the pendant chain. Furthermore, a macromolecular solute containing highly hydrophilic groups, such as  $\text{SO}_3^-$  groups in Nafion, must impose a substantial impact on the molecular structure and dynamics in the solvent. Differential scanning calorimetry studies by Yoshida and Miura<sup>20</sup> and Xie and Okada<sup>21</sup> revealed at least two types of water molecules: mobile and immobilized. The immobilized molecules were supposed to be either strongly bound to  $\text{SO}_3^-$  groups or entrapped in the fluorocarbon backbone.

Molecular dynamics (MD) simulations are proven to be helpful for understanding molecular mechanisms of solvation of macromolecules, provided that reliable force fields are used. In particular, MD studies were successfully applied to solutions of peptides and oligosaccharides.<sup>22–24</sup> However, little work has been done on simulation of hydrated polyelectrolytes so far. Din and Michaelides<sup>25</sup> reported molecular dynamics simulations of diffusion of water and protons in Nafion. The polyelectrolyte was modeled as a network of cylindrical pores of 9.36 and 12.24 Å in diameter with negatively charged walls. Similar simulations of water diffusion in slit-shaped pores of  $\text{Li}^+$  Nafion were performed by Dyakov and Tovbin.<sup>26</sup> Vasyutkin et al.<sup>27</sup> performed semiempirical molecular orbital calculations of heat of water sorption in Nafion and energy barrier of  $\text{H}^+$  and  $\text{Li}^+$  ion exchange between neighboring  $\text{SO}_3^-$  group in a hydrated membrane.<sup>27</sup> Ennari et al.<sup>28</sup> have recently reported atomistic

level molecular modeling of poly(ethylene oxide)sulfonic acid in water. The conductivity of the total system as well as diffusion coefficients for water, proton, and sulfonic anion were found in a reasonable agreement with the experiment. Ljubartsev and Laaksonen<sup>29</sup> studied solvation of DNA in the presence of different counterions ( $\text{Li}^+$ ,  $\text{Na}^+$ ,  $\text{Cs}^+$ ). They found qualitative differences in behavior of counterions. The observed differences in ion binding to DNA may explain different conformational behavior of DNA. Calculated self-diffusion coefficients were found in a good agreement with those obtained from NMR studies. Paddison and Zawodzinski<sup>30</sup> performed ab initio molecular modeling of the Nafion side chain. They determined optimized geometry of the side chain in  $\text{H}^+$  form and preferential position for the water molecule near the  $\text{SO}_3^-$  group. Rotational potential energy surfaces were calculated in order to estimate the flexibility. However, since the molecules of the solvent form readily hydrogen bond to oxygens of the  $\text{SO}_3^-$  group, which serve as hydrogen bond acceptors, the side chain is not expected in solution to show the conformation optimized in a vacuum. It should also be noticed that practically all studies of perfluoro-sulfonic polyelectrolytes consider sorption of water and interaction of the polymer with water, despite the obvious importance of the other solvents, methanol in particular, for fuel cells and selective polyelectrolyte membranes.

In this paper we present a static energy optimization of Nafion oligomer in  $\text{Na}^+$  form in a vacuum and molecular dynamics simulation of solvation of Nafion in water and methanol. The molecular model of the oligomer was built on the basis of the experimental and ab initio studies of perfluoroalkanes and sulfuric acid. Water and methanol were presented by three-center potentials. Analysis of the conformational structure and dynamics has been performed together with a detailed investigation of the solvent structuring. The latter was characterized by radial distribution functions (RDF) and spatial distribution functions (SDF)<sup>31</sup> in three dimensions. In addition, we have studied formation and breakup of hydrogen bonds between the side chain and the molecules of the solvent, their spatial arrangement and stability.

## Simulations

Atomistic model of the monomer unit of Nafion was built using Cerius2 software package from Molecular Simulations, Inc. Since most of the experimental studies of hydrated Nafion were performed for Nafion 1200, we have chosen  $n = 7$ , resulting in equivalent molecular weight of 1165 in the  $\text{H}^+$  form. Our model of the Nafion oligomer was based on the DREIDING force field.<sup>32</sup> The total potential energy of the system was represented as a sum of Lennard-Jones, Coulombic, and bonded terms, coming from covalent angle bending and out-of-plane angle distortions. All covalent bonds were supposed to be rigid. Correspondingly the contribution to the potential energy coming from bond stretching was omitted in this work. The equilibrium bond distances  $R_{ij}^0$  for DREIDING force field were predicted from bond radii of individual atoms using a simple combination rule.<sup>32</sup> Equilibrium covalent angles were assumed to depend on the type of the central atom only. For the simulation reported here, we modified the equilibrium bond distances and angles according to the experimental and ab initio data on perfluoroalkanes, perfluoroethers, sulfonic acid, and dimethylsulfoxide.<sup>33–36</sup> The values of the bond distances and angles are shown in Table 2. The torsional potential for the fluorocarbon backbone was calculated by the density functional theory in ref 37. The results of these calculations were used by Cui et al.<sup>38</sup> in Gibbs ensemble Monte Carlo simulations of vapor–liquid equilibrium of per-

**TABLE 1: Lennard-Jones Parameters for Nafion**

atom	$\sigma$ , Å	$\epsilon$ , kJ/mol
C	3.473	0.3981
F	3.093	0.3035
S	3.550	1.0465
O2, O4	3.07	0.7117
O3, O4, O5	3.15	0.8372

**TABLE 2: Geometry Parameters for Nafion**

Covalent Bonds, Å			
C—C	1.602	C—S	1.80
C—F	1.370	S—O	1.49
C—O	1.380		
Covalent Angles, deg			
CCC	109.6	CCS	112.6
CCF	109.7	FCS	110.7
CCO	109.5	CSO	106.75
COC	109.5	OSO	115.0

fluoroalkanes, and a good agreement with the experimental data was obtained. In our simulation this potential was used to represent CCCC dihedral angles of the skeleton. Correspondingly, FCCF and FCCC dihedrals were disregarded. For the side chain, the DREIDING torsional potential was employed.

The Lennard-Jones parameters (Table 1) were taken from successful simulations of smaller molecules, which contain the same groups as Nafion.<sup>35,37,38</sup> For carbons and fluorines we used the Lennard-Jones parameters from ref 39, where a good agreement between calculated and experimental properties of liquid difluoromethane was achieved. Parameters for sulfur and oxygen in sulfone groups from the recent simulation of Na<sub>2</sub>-SO<sub>4</sub> in water,<sup>35</sup> were used. OPLS parameters were assigned<sup>40</sup> to the ester oxygens. Similar to the usual approach to assigning the nonbonded parameters for the OPLS force field, the structure of the Nafion monomer was divided into smaller fragments. Each of the fragments was made electroneutral. Then, the partial charges for each of the fragments were obtained using the Gasteiger<sup>41</sup> procedure, and equilibrated to yield the total charge of  $e^-$  per monomer unit. The partial charges for skeleton carbons and fluorines are close to those used in ref 39, taking in account that hydrogen atoms of difluoromethane are positively charged. The charges on sulfone oxygens are substantially lower in absolute value than  $e^-$ , used for SO<sub>4</sub><sup>2-</sup><sup>35</sup> and close to those used by Ennari et al.<sup>28</sup> The perfluoroalkane skeleton was terminated by two dummy carbon atoms, which had zero charge and Lennard-Jones energy constant.

The molecule of water was presented by SPC/E potential of Berendsen et al.<sup>42</sup> This three-center model provides a good agreement with experimental data on density, potential energy, and molecular mobility in bulk water at ambient conditions. The molecule of methanol was also described by the three-center potential of van Leuwen and Smit,<sup>43</sup> which provides the best fit to experimental vapor–liquid phase diagram for the pure liquid. Sodium ion was considered as a charged Lennard-Jones particle.<sup>44</sup>

The models of Nafion oligomers composed of 10 and four monomer units were constructed using the polymer builder of Cerius2 and optimized with the Cerius2 energy minimizer. The conjugate gradient method with the maximum atomic displacement of 0.1 Å was used for minimization. The MD simulations were carried out at  $T = 298$  K, both in water and methanol. Lennard-Jones and electrostatic potentials were cut off at 14 Å. In account for long-range electrostatic interactions, the Ewald summation was applied. All covalent bonds were kept rigid using the SHAKE algorithm.<sup>45</sup> The temperature and pressure were maintained by the Nose–Hoover thermostat.<sup>46,47</sup> The

equations of motion were solved by the Verlet scheme<sup>48</sup> with time step of 1 fs. MD simulations were carried out using MDynaMix software package<sup>49</sup> on Silicon Graphics Octane 300 workstation. Gopenmol program was used for visualization of the results.

In the initial configurations of MD simulations the oligomer molecule was placed in a cavity, surrounded by 1024 solvent molecules, arranged as a face centered cubic lattice at a low density of 0.4 g/cm<sup>3</sup>. During the first 10 ps of the trajectories cubic simulation box was gradually squeezed to a density of 0.8 g/cm<sup>3</sup>. Squeezing was followed by a 40 ps NVT simulation with the oligomer molecule kept rigid, to establish preliminary equilibrium in the solvent. Then the simulation was carried out in the NPT ensemble at  $P = 1.0$  atm. Both simulations reached an equilibrium state within first 100 ps of the simulation. The equilibrium densities were 1.11 g/cm<sup>3</sup> in water and 0.842 g/cm<sup>3</sup> in methanol. As expected, these values are somewhat higher than those for the bulk water and methanol obtained with the same models: 0.99<sup>42</sup> and 0.783,<sup>43</sup> respectively. The total length of the simulations was 600 ps for both solvents. Statistics were collected over last 400 ps of each simulation. Every 40 fs the configuration of the whole system was saved for further analysis, which was performed with the TRANAL program of MDynaMix package.

## Results and Discussion

**Structure of the Polytetrafluoroethylene Skeleton.** The characteristic conformations of perfluorosulfate oligomers in a vacuum have been studied using the conjugate gradient algorithm with maximum atom displacement of 0.1 Å, implemented in Cerius2. First, to verify the force fields and to get a better understanding of most favorable conformations of fluorocarbon chains, we performed static energy optimization on  $n$ -perfluoroalkanes up to perfluorooctane. In agreement with the results of density functional calculations by Dixon and Van-Catledge,<sup>37</sup> trans conformations in respect to CCCC dihedral angles are preferential for  $n$ -perfluoroalkanes up to C<sub>8</sub>. For  $n$ -perfluorooctane in particular, the global energy minimum corresponds to the stretched conformation, with all CCCC torsions in trans position. Energy of the oligomer molecule composed of 10 Nafion monomer units in a vacuum was started from two different configurations. In the first configuration all CCCC dihedral angles of the perfluorocarbon skeleton were set to trans conformation. This starting configuration was prompted by our preliminary calculations on  $n$ -perfluoroalkanes. Energy minimization started from this stretched configuration with the distance between the dummy carbon atoms, terminating the perfluorocarbon backbone, equal to 193.45 Å, led to the configuration, shown in Figure 2a. Since the most of the CCCC dihedrals of the skeleton keep trans conformations, the geometry of the oligomer is stretched with the tortuosity of 2.4. Tortuosity was measured as the inverse ratio of the distance between the two dummy carbons, terminating the oligomer to the maximum length possible, corresponding to the completely stretched all-trans conformation. In the other initial conformation the skeleton dihedral angles were randomly distributed over trans and two gauche conformations. Optimization started from the random configuration led to another potential minimum shown in Figure 2b. This is a strongly folded spiral-type configuration has the potential energy 10.2 kcal/equiv lower than the one obtained from the stretched configuration. Nevertheless, most of the skeleton CCCC dihedrals show trans conformation. Potential energy minimization of the four-unit oligomer, started from the stretched configuration, also led to a folded spiral-like structure



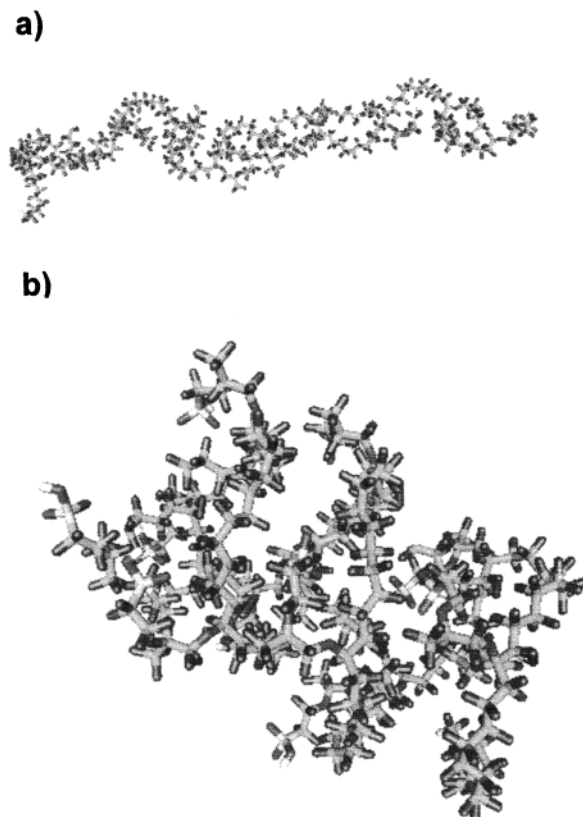


**Figure 2.** Optimized structures of ten-unit perfluorosulfate oligomer obtained by potential energy minimization in a vacuum (a) stretched conformation with tortuosity of 2.4, obtained from the regular configuration with all CCCC dihedrals in trans position, (b) strongly folded spiral-like configuration obtained from a random structure.

(Figure 3a). The folding is caused by intramolecular van der Waals and electrostatic interactions, which turned out to be strong enough to overcome the gain of the torsional potential energy due to folding. None of the optimized structures shown in Figures 2 and 3a are likely to represent the global minimum of the potential energy of the oligomers in a vacuum. However, this analysis shows that even in a vacuum molecular geometry of the oligomers is not entirely dominated by the torsional term. In solution, the intramolecular nonbonded interactions compete to the intermolecular solute–solvent interactions, which favor to stretching of the oligomer. However, the intramolecular entropic contribution to the free energy always favors to folded structure of chain molecules; for example, this effect is well documented for lipid membranes.<sup>50</sup> The three main contributions to the free energy of conformational transition of a macromolecule in solution are (1) intramolecular terms, (2) change in the enthalpy of solvent–solute interactions, and (3) change in the enthalpy and entropy of the solvent. The latter is especially important for hydrophilic molecules in self-associated solvents such as those considered in the present work. This term cannot be correctly taken into account in static simulations, like energy minimization. On the one hand, water shows more extensive hydrogen bond network compared to methanol. On the other hand, methanol is expected to show stronger van der Waals interactions with the hydrophobic polytetrafluoroethylene skeleton of Nafion. Thus, methanol is a better solvent for Nafion; i.e., in a solvated Nafion membrane, the microphase segregation is more pronounced in the case of water.

It should be noted, also, that the energy barriers of conformational transitions in condensed phases are much higher compared to those in a vacuum. In the dense membrane matrix

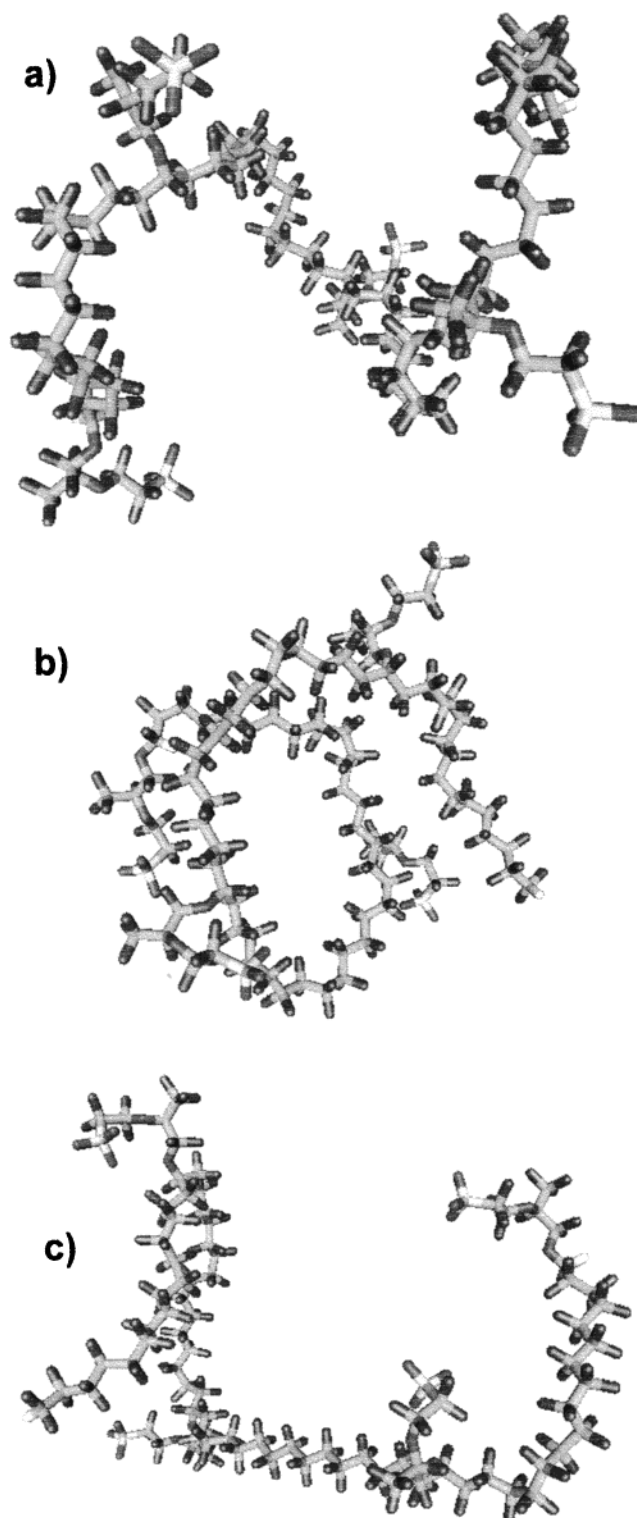


**Figure 3.** (a) Structure of four-unit perfluorosulfate oligomer, optimized in a vacuum (b) snapshot of the molecular configuration of the four-unit oligomer in water and (c) the same in methanol.

of Nafion conformational transitions in polymer chains are sterically hindered. Therefore, Nafion chains in the membrane matrix are not supposed to exhibit the conformations similar to those observed for the oligomers in a vacuum. Yet, the energy minimization in a vacuum allows one to compare different intramolecular contributions into the total internal energy of the system.

In our molecular dynamics simulations of the four-unit oligomer in water and methanol, the fluorocarbon skeleton

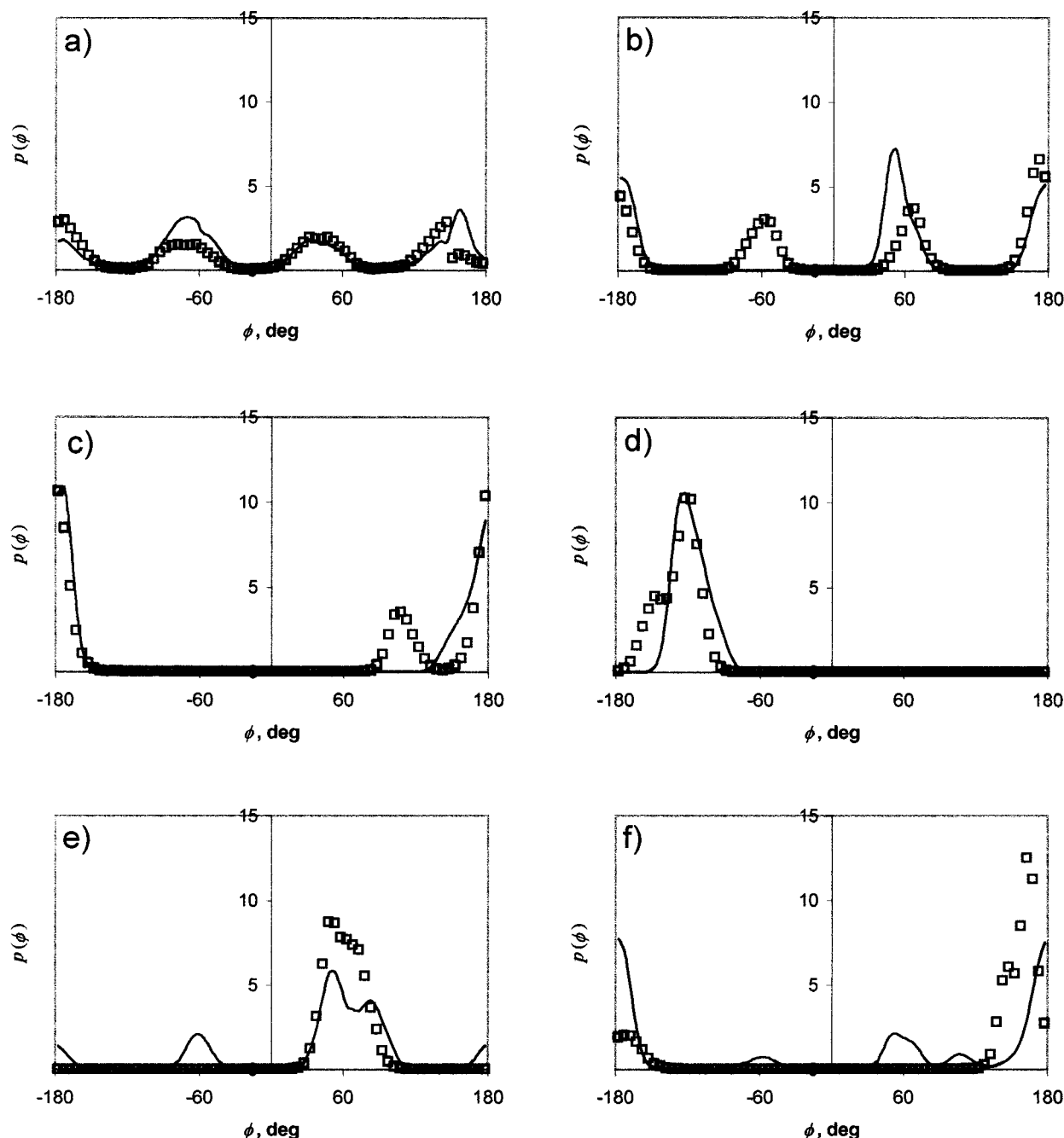


**Figure 4.** Distribution of dihedrals of the side chain averaged over the four side chains of the oligomer in water (lines) and methanol (squares). (a) C4-C5-S-O5, (e) O2-C4-C5-S, (c) C2-O2-C4-C5, (d) C1-C2-O2-C4, (e) O1-C1-C2-C3, (f) C0-O1-C1-C2.

showed preference to trans conformations over CCCC torsions in both solvents. However, the structure of the oligomer in water (Figure 3b) turned out to be substantially more folded compared to that in methanol (Figure 3c) as well as to the initial configuration, optimized in a vacuum (Figures 3a). In average, every third CCCC torsion was found in gauche conformation in water, while in methanol the ratio of the number of gauche and trans CCCC torsions was roughly 1:6, i.e., the oligomer exhibits more stretched structure in methanol, which is clear from Figure 3. Note that the equilibrated conformation of the oligomer differs substantially from the initial one (Figure 3a), which allows us to assume that the impact of the original conformation is not important.

**Geometry of the Side Chain.** Optimized structure of the pendant chain is shown in Figure 1b. This structure is in general similar to the one obtained in RHF calculations of Paddison

and Zawodzinski.<sup>30</sup> Most of the main angles were found in the conformations qualitatively the same as those obtained in ref 30. Namely, we observe trans conformations for CO-O1-C1-C2, O1-C1-C3-C3, C2-C2-C4-C5 dihedrals and gauche conformation for C1-C2-O2-C4 torsion. The O2-C4-C5-S angle makes the only major difference (we observed trans conformation of this dihedral while gauche conformation was obtained in ref 30). As is seen from the snapshots of the oligomer configurations in Figure 2b,c, the distance between the SO<sub>3</sub><sup>-</sup> groups of the neighboring side chains is enough to allow us to consider the behavior of different chains to be independent. In accord with predictions of Paddison and Zawodzinski,<sup>30</sup> the side chain turned out to be relatively stiff. Figure 4 shows the distribution of the six dihedral angles of the side chain, average of four side chains of the oligomer. SO<sub>3</sub><sup>-</sup> groups exhibited fast rotation around S-C5 bond. Note the split

peak of the distribution, reflecting the shape of the torsional potential. The distribution of S–C5–C4–O2 torsional angle has three peaks for methanol and two peaks for water taken as solvent. It is worth mentioning that our simulations are limited in time and might be shorter or comparable with the relaxation time of the side chain. So the existence of several peaks does not necessarily indicate the rotation over a bond; it may also reflect different behavior of different side chains throughout the simulation. In the case of O2–C4–C5–S dihedral, no rotation around C4–C5 bond was observed throughout the recorded trajectories: this dihedral angle turned out to be stiff. A few conformational transitions over O1–C1 and C1–C2 bonds were detected in the simulation with water as a solvent, one transition from distorted trans to trans conformation over C4–O2 bond was detected in the simulation with methanol. All other dihedrals turned out to be pretty stiff and did not show any substantial flexibility within 400 ps of the recorded trajectories. C1–O2–C2–C4 angle is substantially distorted to the position between trans and gauche, conformations. The most frequently observed structure of the side chain is, in general, in accord with the one obtained optimized by energy minimization in a vacuum. Since the side chain was stiff and no reliable statistics on conformational transitions were collected, it is difficult to compare in detail the conformational behavior of the side chain in water and methanol. Still, we can notice that more pronounced mobility of the base of the side chain, reflected in a larger number of conformational transitions noted was detected when water was used as a solvent.

**Solvation of the Side Chain.** In our simulation, the distance between the neighboring sulfone group is sufficient enough to consider solvation shells of each side chain to be independent from the others. Also, due to low concentration of  $\text{Na}^+$  ions in the solution, their impact on the solvation of Nafion side chain can be neglected. This is unlikely to be the case in solvated Nafion membranes. For example, according to the predictions of Girke's theory, water forms clusters of ca. 30 Å in diameter, surrounded by ca. 70  $\text{SO}_3^-$  groups and, correspondingly, 70 positively charged ions. In this case side chains and ions must cumulatively impose strong anisotropic structuring on the solvent water in the clusters. Whatever the shape of the solvent associates is, the structuring of the solvent in a solvated Nafion membrane must be substantially stronger compared to our observations, described below. However, the simulation of the single short oligomer, reported in this paper, should reveal the main features of the solvent structure around the side chains in water and methanol.

Radial distribution functions between the solvent oxygens and different atoms in the side chain show that only  $\text{SO}_3^-$  group of the side chain is strongly hydrophilic while all other fragments of the side chain, including ester-like O1 and O2 atoms, are hydrophobic (Figure 5). This result is in agreement with predictions of Paddison and Zawodzinski.<sup>30</sup> The first peaks on S– $\text{O}_{\text{solvent}}$  and  $\text{O}_{\text{SO}_3}$ – $\text{O}_{\text{solvent}}$  distribution functions are higher for methanol. However, the total number of the solvent oxygens in the first solvation shell of  $\text{SO}_3^-$  group, calculated from S– $\text{O}_{\text{solvent}}$  distribution functions, is close for both solvents: 10.6 for methanol and 12.5 for water, for the number density methanol being lower. Naturally, the solvent molecules in the first solvation shell tend to form hydrogen bonds with negatively charged oxygens of the  $\text{SO}_3^-$  group. For  $\text{Na}^+$  form of Nafion, the  $\text{SO}_3^-$  group can serve only as an acceptor of a hydrogen bond donated by a solvent molecule. In our simulation hydrogen bonds were considered implicitly, i.e., no special energy term for hydrogen bonding was applied. For the purpose of counting,

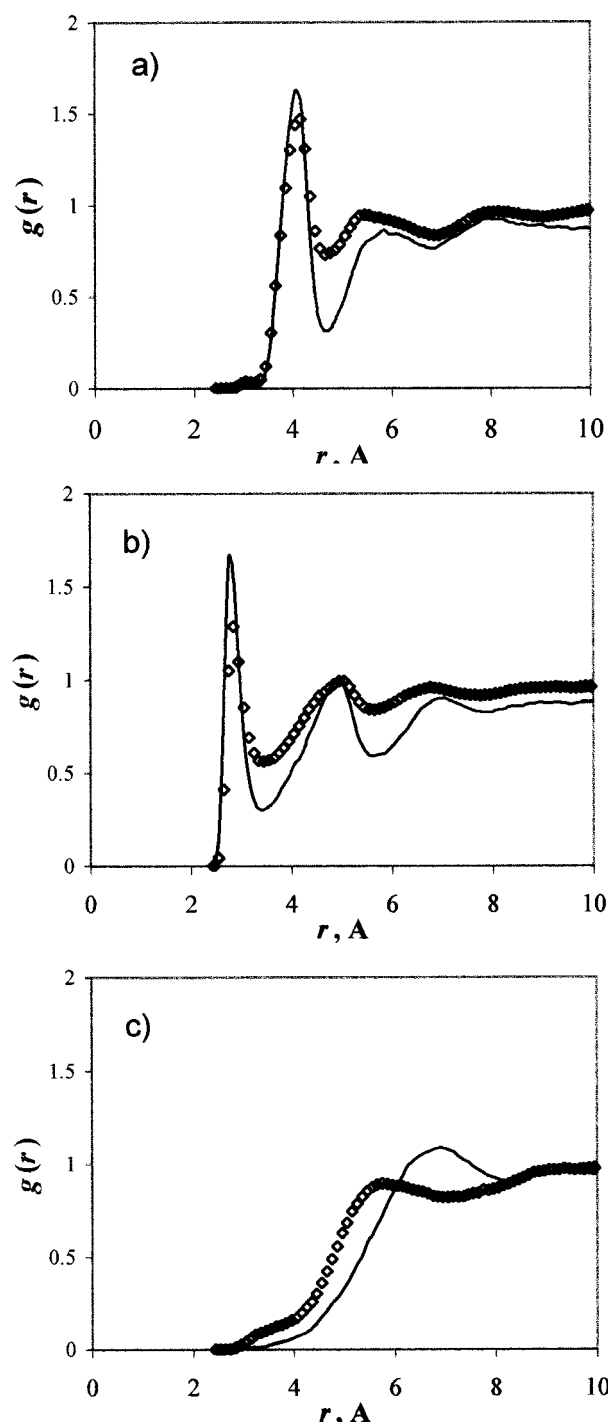


**Figure 5.** Radial distribution functions for pairs formed by atoms of the side chain and oxygen atoms of water (lines) and methanol (diamonds). (a) S– $\text{O}_{\text{solvent}}$ , (b)  $\text{O}_{\text{SO}_3}$ – $\text{O}_{\text{solvent}}$ , (c)  $\text{O}_2$ – $\text{O}_{\text{solvent}}$ .

we used a geometry criteria of hydrogen bonding: two oxygens atoms are considered to form a hydrogen bond via a hydrogen atom, if the distance between the oxygens does not exceed 3.4 Å, while OHO angle exceeds 120°. With these criteria the oxygens of one  $\text{SO}_3^-$  group were found to form 5.1 for water and 3.7 for methanol in average. We explain less extensive hydrogen bonding in the case of methanol by steric factors, because methanol molecules are larger than the molecules of water. Stability of the hydrogen bonds is characterized by hydrogen bond lifetime. Since a hydrogen bond is a three-atom interaction, calculation of hydrogen bond lifetime with a geometry criteria are time-consuming. Moreover, hydrogen bonds are known to be flexible and development of reliable



geometry criteria for lifetime estimation is problematic. In this work we analyze hydrogen bond lifetime in terms of residence times for oxygen atoms. This approach was applied to study hydrogen bonding of water to disaccharides<sup>23</sup> and DNA.<sup>29</sup> We assumed a hydrogen bond between a molecule of the solvent and  $\text{SO}_3^-$  group of Nafion to be established, when the distance between two oxygen atoms belonging to solvent molecules and an oxygen of a  $\text{SO}_3^-$  group remains shorter than 3.4 Å within 2 ps. The hydrogen bond was considered to be broken, when this distance exceeds 3.55 Å or when it remains larger than 3.4 Å within 2 ps. Estimation of the residence times was based on the assumption that the probability of a hydrogen bond to be destroyed within time  $t$  can be presented as  $1 - a \exp(-bt)$ .

With these criteria, we obtained solute–solvent hydrogen bond lifetimes of 8.3 ps for water and 12.2 ps for methanol. Subsequently, the hydrogen bonds between the solvent and Nafion remain stable within several rotation times of individual molecules in the bulk liquids. As compared to water, methanol forms more stable hydrogen bonds with  $\text{SO}_3^-$  groups of Nafion, although the overall translation diffusion coefficient of the solvent molecules in the system ( $1.77 \times 10^{-9}$  and  $1.80 \times 10^{-9}$  m<sup>2</sup>/s in water) were found to be very close to each other and slightly lower than the diffusion coefficients in the corresponding bulk liquids. It is worth noticing that a water molecule, which donates a hydrogen bond to  $\text{SO}_3^-$  group, is able to donate another hydrogen bond to another water molecule and accept two hydrogen bonds from the solvent water, while methanol is able only to accept one hydrogen bond donated by another methanol molecule. Thus, methanol molecules, hydrogen-bonded to the  $\text{SO}_3^-$  group, have roughly 3 times lower ability to participate in hydrogen bond network of the solvent in general. This allows us to assume that the side chain produces weaker impact on the structure of solvent methanol compared to water. The longer lifetimes of the solvent–solute hydrogen bonds in the case of methanol also show that the solvent molecule involved in a hydrogen bond with the side chain is less involved in the overall circulation of the solvent in the case of methanol.

The structure formation caused by the interactions of the side chain with the solvent can be demonstrated with three-dimensional spatial distribution functions (SDF). SDF is a three-dimensional density profile, calculated in a reference coordinate system, rigidly attached to the side chain. We built the reference coordinate system on S–O5 and S–C5 vectors. The SDFs obtained for four side chains of the oligomer were averaged. Figure 6 shows the coordinates of the atoms of the side chain in the reference system averaged through the trajectories and the regions where the average local density of the solvent oxygens is 2.2 times as large as the average number density of the solvent. In both cases the first solvation shell is clearly observed. The solvent molecules hydrogen bonded to the sulfogroup forms the first solvation shell. Higher density near the hydrophobic region is due to spatial effects, similar to those known for fluids near walls (e.g., ref 51). However, we did not observe a localization of the solvent molecules in the second solvation shell. Thus, anisotropic structuring, imposed by a single side chain to the solvent, ranges up to ca. 6 Å from the side chain skeleton.

## Conclusion

We have performed molecular mechanics and molecular dynamics simulation studies of perfluorosulfonated oligomers, representing fragments of Nafion membrane. The parameters of the force field for the macromolecule were chosen to

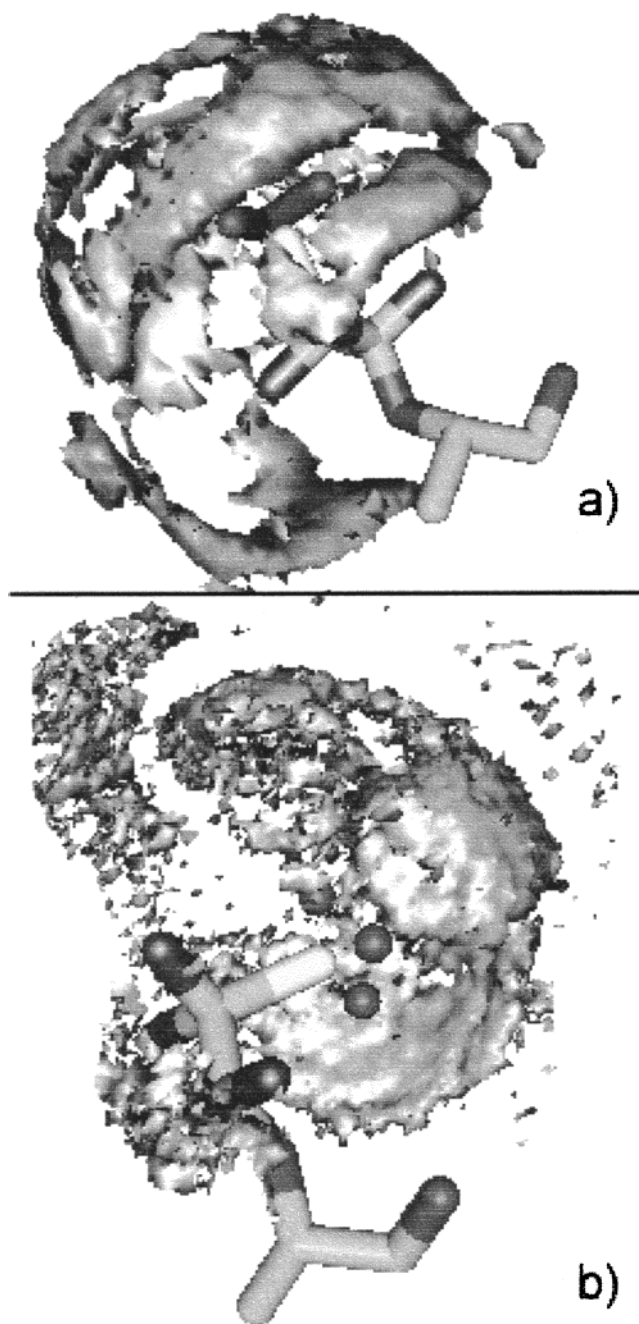


**Figure 6.** Average coordinates of the atoms of the side chain in a reference coordinate system attached to S–O5 and S–C5 vectors and spatial distribution functions of the solvent oxygens around the side chain. Clouds in gray show the regions where the average local density of the solvent oxygens is 2.2 times as large as the average number density of the solvent. (a) water, (b) methanol.

reproduce the experimental data on vapor–liquid equilibrium and self-diffusion for smaller molecules which containing the same groups as Nafion. Potential energy minimization of lower  $n$ -perfluoroalkanes in a vacuum showed preference to the stretched all-trans conformations, in agreement with the density functional studies of Dixon and Van-Cattledge.<sup>37</sup> Energy optimization of the oligomer, composed of 10 monomer units, in a vacuum, led to a stretched geometry of the fluorocarbon skeleton with tortuosity of 2.4, when the regular conformation with all CCCC angles in the trans position was taken as the starting configuration. Started from a randomly bent chain, we came to a highly folded spiral-like configuration. We conclude that the geometry of the skeleton is not entirely dominated by

the torsional contribution to the intramolecular potential energy. In molecular dynamics simulations of the shorter oligomer in water and methanol, we observed a noticeable difference between the geometries of the fluorocarbon skeleton. The structure of the skeleton in water was substantially more folded than in methanol. We can expect considerable dependence of the microstructure of solvated Nafion membranes upon the solvent used.

In general, the side chain of the Nafion oligomer was found to be quite stiff; only a few conformational transitions in the side chain were detected. Both water and methanol formed stable hydrogen bonds with the oxygens of  $\text{SO}_3^-$  group. As expected all other parts of the side chain are hydrophobic, including ester oxygens, which showed practically no tendency to hydrogen bonding. On average, each  $\text{SO}_3^-$  group formed ca. five hydrogen bonds to the solvent water and four bonds to methanol. The solvent molecules bonded to the  $\text{SO}_3^-$  group form a pronounced anisotropic first solvation shell. No substantial localization of the solvent molecules in the second solvation shell was observed. However, the number of hydrogen bonds obtained shows that, due to high concentration of  $\text{SO}_3^-$  groups and ions, the molecular structure of the sorbed solvent in the hydrated membrane must differ dramatically from that in the bulk solvent. For example, in view of predictions of Gierke's theory of ionic clusters, roughly every third water molecule in the cluster forms a hydrogen bond to a side chain. The hydrogen bond lifetimes are found to be several times longer than rotational correlation times of individual solute molecules in the bulk. In the same time, no immobilized molecules strongly bonded to the  $\text{SO}_3^-$  groups were detected.

The force field parametrization performed in the present work is used in ongoing large-scale molecular dynamics simulation studies of solvated Nafion membranes, which will be reported in forthcoming communications.

**Acknowledgment.** Research is supported by the U.S. Army NSC. The authors thank Dr. D. Rivin for stimulating discussion.

## Note Added after ASAP Posting

This article was released ASAP on April 5, 2000, with an incorrect version of the Abstract. The correct version of the Abstract now appears. The correct version was posted April 11, 2000.

## References and Notes

- (1) Takenaka, H.; Torikai, E.; Kawmi, Y.; Wakabayashi, N. *Int. J. Hydrogen Energy* **1982**, *5*, 397.
- (2) Lu, P. W. T.; Srinivasan, S. *J. Appl. Electrochem.* **1979**, *9*, 269.
- (3) Ogumi, Z.; Nishio, K.; Yoshizawa, S. *Electrochim. Acta* **1981**, *26*, 1779.
- (4) Leo, J. M. J.; Mugerwa, M. N. *Fuel Cell Systems*; Plenum Publishing Corp.: New York, 1993.
- (5) Penner, S. S.; Appleby, A. J.; Baker, B. S. *Energy* **1995**, *20*, 331.
- (6) Morris, D. D.; Sun, X. J. *Appl. Polymer Sci.* **1993**, *50*, 1445.
- (7) Yeager, H. L. In *Perfluorinated Ionomer Membranes*; ACS Symposium Series C 180; American Chemical Society: Washington, DC, 1982; p 41.
- (8) Sakai, T.; Takenaka, H.; Torikai, E. *J. Electrochem. Soc.* **1986**, *133*, 88.
- (9) Gierke, T. D.; Hsu, W. L. In *Perfluorinated Ionomer Membranes*; ACS Symposium Series 180; American Chemical Society: Washington, DC, 1982; p 283.
- (10) Escoubes, M.; Pineri, M. In *Structure and Properties of Ionomers*; NATO ASI Series C 198; D. Reidel Publishing: Dordrecht, 1987; p 341.
- (11) Gierke, T. D.; Munn, G. E.; Wilson, F. C. *J. Polym. Sci.: Polymer Phys.* **1981**, *19*, 1687.
- (12) Mauritz, K. A.; Rogers, C. E. *Macromolecules* **1985**, *18*, 483.
- (13) Eikerling, M.; Kornyshev, A. A.; Stimming, U. *J. Phys. Chem.* **1997**, *101*, 10807.
- (14) Pineri, M.; Duplessix, R.; Volino, F. In *Perfluorinated Ionomer Membranes*; ACS Symposium Series C180; American Chemical Society: Washington, DC, 1982; p 249.
- (15) Falk, M. *Can. J. Chem.* **1980**, *58*, 1495.
- (16) Plate, N. A.; Shibaev, V. P. *Brush-Like Polymers and Liquid Crystals*. Khimija: Moscow, 1980; p 304 (Russ. transl.).
- (17) Timashev, S. F. *Physical Chemistry of Membrane Processes*; Khimija: Moscow, 1988; p 237 (Russ. transl.).
- (18) Ozerin, A. N.; Rebrov, A. V.; Yakunin, A. N.; Bessonova, N. P.; Dreiman, N. A.; Sokolov, N. F.; Bakeev, L. F. *Vysokomol. Soedin., Ser. A* **1986**, *28*, 2303.
- (19) Tovbin, Y. K. *Zh. Fiz. Khim.* **1998**, *72*, 55.
- (20) Yoshida, H.; Miura, Y. *J. Membr. Sci.* **1992**, *68*, 1.
- (21) Xie, G.; Okada, T. *J. Chem. Soc., Faraday Trans.* **1996**, *92*, 6636.
- (22) Bruschweiler, R.; Roux, B.; Blackledge, M.; Giesinger, C.; Karplus, M.; Ernst, R. R. *J. Am. Chem. Soc.* **1992**, *114*, 2289.
- (23) Vishnyakov, A.; Widmalm, G.; Kowalewski, J.; Laaksonen, A. *J. Am. Chem. Soc.* **1999**, *121*, 5403.
- (24) Vishnyakov, A.; Widmalm, G.; Laaksonen, A. *Angew. Chem. Int. Ed.* **2000**, *39*, 140.
- (25) Din, X. D.; Michaelidis, E. E. *AIChE J.* **1998**, *44*, 35.
- (26) Dyakov, V. A.; Tovbin, Y. K. *Russ. Chem. Bull.* **1995**, *44*, 1186.
- (27) Vasyutkin, N. F.; Tovbin, Y. K. *Vysokomol. Soedin. Ser. A* **1993**, *35*, 1600.
- (28) Ennari, J.; Elomaa, M.; Sundholm, F. *Polymer* **1999**, *40*, 5053.
- (29) Lyubartsev, A. P.; Laaksonen, A. *J. Biomol. Struct. Dyn.* **1998**, *16*, 597.
- (30) Paddison, S. J.; Zawodzinski, T. A. *Solid State Ionics* **1998**, *113*–*115*, 333.
- (31) Bergman, D. L.; Laaksonen, L.; Laaksonen, A. *J. Mol. Graph. Model.* **1997**, *15*, 301.
- (32) Mayo, S. L.; Olafson, D.; Goddard, W. A. *J. Phys. Chem.* **1990**, *94*, 8897.
- (33) Gallaher, K. L.; Yokozeki, A.; Bauer, S. H. *J. Phys. Chem.* **1974**, *78*, 2389.
- (34) Gejji, S. P.; Hermansson, K.; Lindgren, J. *J. Phys. Chem.* **1993**, *97*, 3712.
- (35) Cannon, W. R.; Pettitt, B. M.; McCammon, J. A. *J. Phys. Chem.* **1994**, *98*, 6225.
- (36) Thomas, R.; Showemaker, C. B.; Eriks, K. *Acta Crystallogr.* **1966**, *21*, 12.
- (37) Dixon, D.; Van-Catledge, F. A. *Intermed. J. Supercomput. Appl.* **1988**, *2*, 62.
- (38) Cui, S. T.; Siepmann, J. I.; Cochran, H. D.; Cummins, P. T. *Fluid Phase Equilib.* **1998**, *146*, 51.
- (39) Jeldovszky, P.; Mezei, M. *J. Chem. Phys.* **1999**, *110*, 2991.
- (40) Jorgensen, W. L.; Maxwell, D. S.; Tirado-Rives, J. *J. Am. Chem. Soc.* **1996**, *118*, 11225.
- (41) Gasteiger, J.; Marsili, M. *Tetrahedron* **1980**, *36*, 3219.
- (42) Berendsen, H. J. C.; Grigera, J. R.; Straatsma, T. P. *J. Phys. Chem.* **1987**, *91*, 6269.
- (43) Van Leeuwen, M. E.; Smit, B. *J. Phys. Chem.* **1995**, *99*, 1831.
- (44) Heinzinger, K. *Phys. B* **1985**, *131*, 196.
- (45) van Gasteren, W. F.; Berendsen, H. J. C. *Mol. Phys.* **1977**, *34*, 1311.
- (46) Nose, N. *Mol. Phys.* **1984**, *52*, 255.
- (47) Hoover, W. G. *Phys. Rev A* **1985**, *31*, 1695.
- (48) Verlet, L. *Phys. Rev.* **1967**, *159*, 98.
- (49) Lyubartsev, A.; Laaksonen, A. *A Scalable Parallel General-Purpose Simulation Software for Arbitrary Mixtures of Molecules*. Stockholm University: Stockholm, 1998. See URL: [http://www.fos.su.se/physical/sasha/md\\_prog.html](http://www.fos.su.se/physical/sasha/md_prog.html).
- (50) Bloom, M.; Mouritsen, O. G. *The Evolution of Membranes. In Biophysics Handbook on Membranes*; Lipowsky, R., Ed.; Elsevier: Amsterdam, Vol. 1 (*Structure and Conformation*), p 89.
- (51) Vishnyakov, A.; Piotrovskaya, E. M.; Brodskaya, E. N. *Adsorption* **1998**, *4*, 207.